Effects of Molecular Size and Configuration on Diffusion in Microporous Membranes

W. M. DEEN
M. P. BOHRER
and
N. B. EPSTEIN

Department of Chemical Engineering,
Massachusetts Institute of Technology
Cambridge, MA 02139

Effects of molecular size and configuration on hindered diffusion were examined by measuring diffusion of two series of uncharged macromolecules through track-etch membranes with uniform and well-defined pore geometry. At any given Stokes-Einstein radius, diffusivities in small pores were lower for ficoll (crosslinked structure) than for dextran (more nearly linear structure).

SCOPE

The effective diffusivity of a solute within a finely porous medium (e.g., a membrane or porous catalyst support) is frequently found to be less than its value in bulk solution. This phenomenon is known as "hindered" or "restricted" diffusion and it arises fundamentally from the fact that the characteristic dimension of the solute molecule is no longer small compared to that of the pore through which it passes. Several theoretical descriptions of liquid-phase mass transfer in fine pores have been developed based on hydrodynamic models of diffusion. These generally treat the membrane or other finely porous structure as an array of identical cylindrical pores, and the solute molecules as solid spheres. The advantages of such physical models over phenomenological approaches, such as that based on nonequilibrium thermodynamics, is that they offer the possibility of predicting mass transfer rates from a limited number of independently measurable properties of the solute and porous barrier, or alternatively, allow structural or other inferences to be made regarding the transport barrier when transport rates are known.

The development in recent years of track-etch membranes has provided an excellent model system with which to test theories of hindered diffusion. These membranes are generally formed from thin sheets of mica or polycarbonate, with pores created by a two step process of bombardment with heavy fission fragments followed by chemical etching. The resultant pore geometry is highly regular and closely resembles the idealized cylindrical pores considered in the theories. These membranes have been employed in several previous investigations of restricted diffusion, but data remain somewhat limited. One objective of the present study was to extend the available data on diffusion of uncharged solutes to include substantially higher ratios of molecular size to pore size than had been considered previously, for comparison with existing theory. A second objective was to examine the effects of molecular configuration on restricted diffusion, for which little theoretical analysis is available. This was done by measuring diffusion of dextran, a slightly branched polysaccharide, and ficoll, a crosslinked copolymer of sucrose and epichlorohydrin, over a wide range of molecular sizes in polycarbonate track-etch membranes.

CONCLUSIONS AND SIGNIFICANCE

Measurements of bulk solution diffusivity (D_∞) performed in membranes with large pores revealed that the tritiated dextran and ficoll used in this study have Stokes-Einstein radii ranging from about 2.3-6.0 nm and 1.6-3.5 nm, respectively. This was taken as the measure of molecular size. Characterization of two polycarbonate membranes of the smallest commercially available pore size indicated pore radii of 7.48 and 8.75 nm, at or slightly above the nominal pore radius of 7.5 nm. Thus, hindered diffusion could be examined at ratios of molecular size to pore size as high as 0.77. The results of hindered diffusion experiments in these membranes are summarized in Figure 5. Pore-to-bulk solution diffusivity ratios (D/D_∞) for dextran greatly exceeded those for ficoll over the entire range of molecular sizes studied. These results are in accord with other data in the literature suggesting less hindrance to transport of nearly linear polymers than globular polymers, in a variety of porous media.

Available theoretical results, shown by the solid and dashed curves in Figure 5, do not provide particularly accurate predictions for either series of macromolecules. As might have been anticipated, the hard sphere theories are in substantially better agreement with the data for ficoll than that for dextran. These results demonstrate the need for theoretical analysis based on more realistic models of permeating macromolecules, including probably effects of both molecular shape and deformability. To the extent that differences in molecular flexibility may explain the relative diffusion rates of dextran and ficoll, this mechanism is not dependent on shear-induced deformation of the macromolecules within pores, since transmembrane water flow was absent.

Correspondence concerning this paper should be addressed to W. M. Deen.
M. P. Bohrer is presently with Bell Laboratories, Room 6F-317, 600 Mountain Ave., Murray Hill, NJ 07974.

0001-1541-81-4912-0952-$2.00.

INTRODUCTION

Hydrodynamic theories of mass transfer in fine pores have been applied to diffusive and convective transport across synthetic and biological membranes (Beck and Schultz, 1972; Malone and Anderson, 1978; Deen et al., 1979), diffusion in porous glass (Colton et al., 1975), and separation processes such as hydrodynamic chromatography (Prieve and Hoysan, 1978; Silebi and McHugh, 1978) to cite a few examples. Several useful discussions of the development of these theories are those given by Bean (1972), Anderson and Quinn (1974), Brenner and Gaydos (1977) and Malone and Anderson (1978). The simplest model for a porous medium is generally employed, in which transport is viewed as taking place through numerous, identical cylindrical pores. If the molecules of solute are sufficiently larger than those of the solvent, they may be treated as particles having both Brownian and hydrodynamic characteristics, while the solvent may be viewed as a continuum. In the absence of constraints introduced by pores, this leads to the well known result of Einstein:

$$D_\infty = \frac{kT}{f_\infty} \tag{1}$$

For the special case of a solid sphere, where Stokes' result is $f_\infty = 6\pi\mu a$, the familiar Stokes-Einstein equation is obtained.

The apparent diffusivity in a pore (D) is defined here with reference to the (measurable) solute flux averaged over the pore cross-sectional area. Within pores of dimensions comparable to that of a solute molecule, it is generally found that $D/D_\infty < 1$. This may be interpreted as the combined result of: (1) an increase in the hydrodynamic drag above f_∞, due to the pore wall; and (2) nonhydrodynamic interactions between the solute and pore wall, expressible as potentials. The simplest such interaction is the hard sphere type, in which the sphere center is "sterically excluded" from an annular region next to the pore wall equivalent to its radius. In this case, D/D_∞ is given by (Anderson and Quinn, (1974):

$$\frac{D}{D_\infty} = 2\int_0^{1-\lambda} [f_\infty/f(\lambda,\beta)]\beta d\beta$$

$$= \phi \frac{\int_0^{1-\lambda} [f_\infty/f(\lambda,\beta)]\beta d\beta}{\int_0^{1-\lambda} \beta d\beta} \tag{2}$$

$$\phi = (1-\lambda)^2$$

In the second form of Eq. 2, D/D_∞ is written as the product of an equilibrium partitioning coefficient (ϕ) and the average of f_∞/f over the "accessible" cross-sectional area. Little use has been made of Eq. 2 without approximation since off-axis values of f are available only for $\lambda << 1$. It is usually assumed that $f^{-1}(\lambda, 0)$ adequately approximates the required average value of $f^{-1}(\lambda, \beta)$, leading to:

$$\frac{D}{D_\infty} \simeq \phi \frac{f_\infty}{f(\lambda, 0)} \tag{3}$$

Values of $f(\lambda, 0)$ have been tabulated by Paine and Scherr (1975), among others. For $\lambda << 1$, the integrals in Eq. 2 have been evaluated using asymptotic results for small spheres (Brenner and Gaydos, 1977):

$$\frac{D}{D_\infty} = 1 + \frac{9}{8}\lambda\ln\lambda - 1.54\lambda + 0(\lambda) \tag{4}$$

For electrically charged solutes and/or pores, electrostatic interactions between solute and pore wall are important, and modifications in Eqs. 3 and 4 are required (Malone and Anderson, 1978; Smith and Deen, 1980).

DEXTRAN

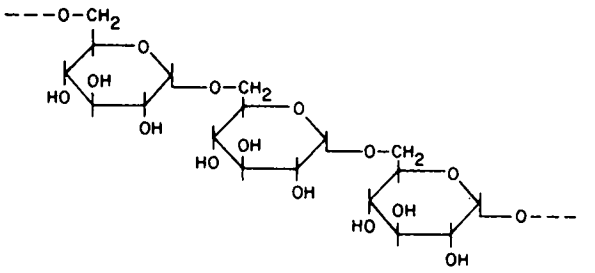

FICOLL

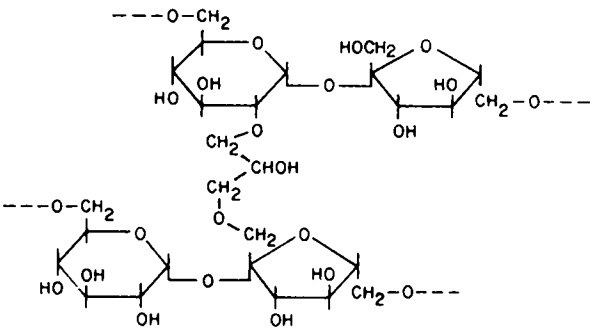

Figure 1. Partial structures of dextran and ficoll.

The development of the track-etch process for making membranes of well-defined pore geometry (Price and Walker, 1962) has made possible quantitative tests of Eqs. 3 and 4 in structures where pore radius is uniform and can be determined independently of hindered diffusion measurements. In perhaps the most definitive experimental study of hindered diffusion of uncharged solutes, Beck and Schultz (1972) measured diffusion rates of urea, glucose, sucrose, α- and β-dextrin and ribonuclease, through track-etch mica membranes. A good fit of the experimental data was obtained using Eq. 3, although results were limited in that almost all data were for solute and pore sizes such that $\lambda < 0.2$. Less satisfactory agreement with Eq. 3 was obtained in a more limited study by Van Bruggen et al. (1974) using track-etch polycarbonate membranes. For several solutes with $\lambda \leq 0.1$, D/D_∞ was lower than that predicted by Eq. 3. For diffusion of bovine serum albumin in mica membranes with $\lambda = 0.19$, Wong and Quinn (1976) found D/D_∞ to be one-half that predicted by Eq. 3. Comparable values were obtained at two different ionic strengths, so that electrostatic factors do not readily explain this discrepancy. Eq. 4, which is presumably more accurate than Eq. 3 for $\lambda << 1$, does predict somewhat lower values of D/D_∞, although not as low as those seen by Van Bruggen et al. (1974) or Wong and Quinn (1976). Additional studies in track-etch membranes using polystyrene spheres (Conlon and Craven, 1972; Malone and Anderson, 1978) do not provide as direct a test of Eqs. 3 and 4, because of the probable or demonstrated influence of electrostatic interactions.

In the present study we extend the available data on hindered diffusion of neutral solutes by examining diffusion of dextran and ficoll in polycarbonate track-etch membranes. As shown by the partial structures in Figure 1, these two water-soluble polymers have distinctly different molecular configurations. The type of dextran we employed is a slightly branched (5% branch points, Granath, 1958) polymer of D-glucopyranose, with most branches containing only one or two monomer units (Larm et al., 1971). Ficoll is a crosslinked copolymer of sucrose and epichlorohydrin, which we infer to

have a structure resembling that in Figure 1. Comparison of diffusion results for these two series of macromolecules provides a test both of Eq. 3 and of the effect of molecular configuration, for which no theory appears to be available.

MATERIALS AND METHODS

Preparation and Fractionation of Macromolecules. Disperse mixtures of macromolecules covering a suitable range of molecular sizes were obtained by mixing commercially available dextran fractions (T10, T20, and T40, Pharmacia Fine Chemicals, Piscataway, NJ) or hydrolyzing high molecular weight ficoll (Ficoll 70, Pharmacia). The dextran and ficoll mixtures were labeled with tritium following a procedure described previously (Chang et al., 1975; Bohrer et al., 1979), involving partial oxidation with sodium periodate followed by reduction with tritiated sodium borohydride. These disperse mixtures of dextran or ficoll were employed in all macromolecule diffusion experiments, data on individual molecular sizes being obtained by fractionating all samples by gel chromatography prior to analysis. Thus, each experiment yielded data for the entire range of molecular sizes considered. Specific activities of the tritiated macromolecules were sufficient to permit use of dilute solutions (total macromolecule concentration < 0.3 g/dL). [Based on partial specific volumes for dextran and ficoll of 0.6-0.7 g/mL (Bohrer et al., 1979), the maximum volume fraction of solute used was $\epsilon = 0.002$. Measured diffusivities should differ from those at infinite dilution by a term of order ϵ (Anderson, 1973), in the present experiments a correction of less than 1%.]

Fractionations were performed on gel columns (total volume ~250 mL) packed with Sephadex G-100 (Pharmacia), using 0.05 N ammonium acetate, pH 7.0, as eluant. Sample size was generally 0.5 mL. Elution volumes of dextran and ficoll were related to molecular size by column calibration using several proteins, as described previously (Chang et al., 1975). This measure of molecular size will be referred to as "column radius," as distinguished from the Stokes-Einstein radius obtained in the diffusion studies to be described.

Membrane Characterization. Polycarbonate track-etch membranes with nominal pore diameters of 0.015 μm, 0.1 μm and 1.0 μm were used as supplied by Nuclepore Corp. (Pleasanton, CA). Each batch of membranes ordered was specified to be hand punched from similar locations on the same production sheet in order to minimize intermembrane variations. Membranes were characterized in terms of three quantities, average pore length (L), pore radius (r), and number density of pores (n). Since the pores of these membranes are essentially uniform circular cylinders (Liabastre and Orr, 1978), pore length is very nearly equal to membrane thickness, exceeding membrane thickness only to the extent that the pores are not aligned normal to the membrane surfaces. Information supplied by Nuclepore indicated that the maximum deviation from the normal is 29°. Assuming all deviations of 0 to 29° to be equally probable, average pore length would exceed membrane thickness by 6.8%. Employing this factor, pore length is determined by weighing a membrane of known area:

$$L = \frac{1.068\ W}{(1 - n\pi r^2)A_T\rho} \tag{5}$$

where the density of polycarbonate is taken to be 1.19 g/cm^3. The denominator includes a correction for membrane porosity ($n\pi r^2$), which is significant for the larger pore sizes used.

The additional measurements required to complete the membrane characterization were obtained from two of the following: scanning electron microscopy, water flow, or diffusion of small solutes. For scanning electron microscopy (Jeolco model JSM-U3) membranes were mounted shiny side up and lightly coated with gold by vacuum deposition. Pore density was determined by counting the number of pores in photographs obtained at 3,000-20,000 × magnification, with the area in view calibrated by photographing diffraction gratings (6,000 lines/cm or 24,000 lines/cm, Ladd Research Industries, Burlington, VT) at the same magnification and angle of view. Satisfactory images were obtained for membranes with nominal pore diameters of 0.1 μm and 1.0 μm, but for the 0.015 μm size there was insufficient resolution for reliable counting of pores.

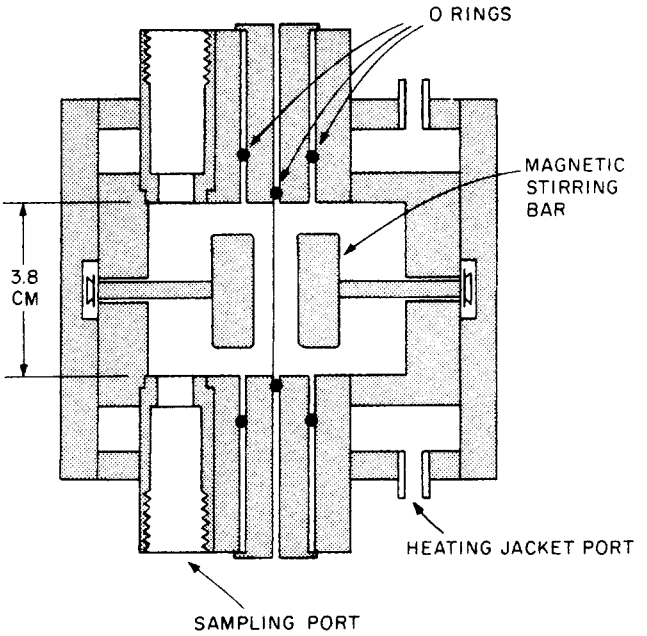

Figure 2. Diffusion cell, drawn to scale. Each half cell contains two heating jacket ports and two sampling ports. The volume of each chamber is 26.9 cm^3 and the exposed membrane area 11.4 cm^2.

The scanning electron micrographs obtained were not suitable for determination of pore radius, which required measurements of hydraulic permeability and/or diffusion of small solutes. Water flow measurements were performed for all three membrane sizes with membranes mounted in the diffusion cell (see below) and hydrostatic pressures ranging from 0.3 to 2.5 kPa. Higher pressures were not used since in preliminary experiments irreversible deformation of some of the unsupported membranes was noted at 4.0 kPa. Flow rates were determined by weighing the filtrate collected in timed intervals (1.0 μm pore diameter) or following the motion of air bubbles introduced into a constant bore glass capillary tube connected to the outlet (0.1 μm and 0.015 μm). At the highest flow rates it was necessary to correct for pressure drops elsewhere in the apparatus, although pore Reynolds number did not exceed 2×10^{-3}. The Poiseuille equation was used to interpret the results:

$$L_p \equiv \frac{Q}{A\Delta P} = \frac{n\pi r^4}{8\mu L} \tag{6}$$

For the 0.015 μm membranes, where scanning electron microscopy could not be used, the quantity $n\pi r^2/L$ was calculated from diffusion measurements with ^{14}C-sucrose, ^{14}C-glucose, or ^{14}C-urea (obtained in crystalline form from New England Nuclear, Boston, MA), as described in the next section.

Diffusion Measurements. The diffusion cell used was machined from lucite and is illustrated in Figure 2. The membrane is supported on its periphery by two annular discs that bolt together, to which are bolted the two half cells. Each half cell is jacketed for temperature control (37.0 ± 0.2°C) and contains two sampling ports. Magnetic stirring bars cemented to stainless steel shafts are mounted internally and driven by rotation of an external magnet. Stirring speed was controlled at 285 ± 5 rpm (Standard Servodyne motor and controller, Cole-Parmer Instrument Co., Chicago, IL). The exposed membrane area is 11.4 cm^2 and the volume of each half cell is 26.9 cm^3

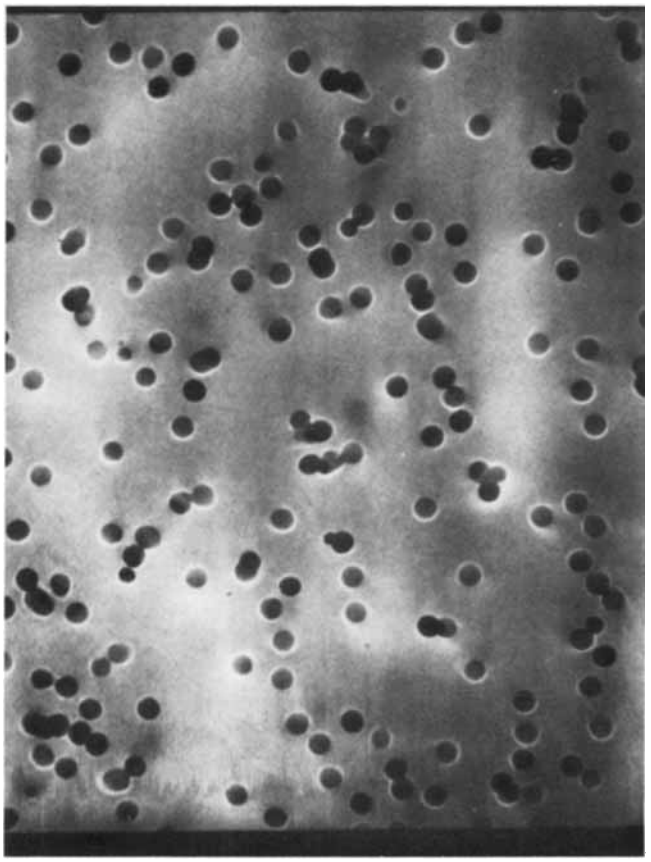

Figure 3. Scanning electron micrograph of a membrane with 1.0μm nominal pore diameter. Magnification is 3000X.

In the batch diffusion experiments conservation of mass indicates that solute concentration in the "downstream" chamber is given by

$$\ln\left[\frac{C_\infty - C}{C_\infty - C_o}\right] = \frac{-2At}{R_T V} \tag{7}$$

In addition to the membrane resistance, the overall mass transfer resistance (R_T) includes that contributed by the boundary layers adjacent to the membrane surfaces, and end effects arising from the fact that near the pore ends, diffusion is not one-dimensional (Malone and Anderson, 1977). Accordingly,

$$R_T = R_m + 2R_b + 2R_e \tag{8}$$

The individual resistances are given by

$$R_m = \frac{L}{n\pi r^2 D} \tag{9}$$

$$R_b = \frac{1}{k} \tag{10}$$

$$R_e = \frac{\pi r/4}{n\pi r^2 D_\infty} \tag{11}$$

As discussed by Colton and Smith (1972), mass transfer coefficients in this geometry follow a correlation of the form

$$\frac{kb}{D_\infty} = \alpha N_{Re}^{\gamma} N_{Sc}^{1/3} \tag{12}$$

The mass transfer coefficient can be seen to vary as $D_\infty^{2/3}$, all other quantities being fixed in our experiments. It is convenient then to rewrite Eq. 8 in the form

$$R_T = \frac{K_1}{D} + \frac{K_2}{D_\infty^{2/3}} + \frac{K_3}{D_\infty} \tag{13}$$

where the constants K_1, K_2, and K_3 relate to the membrane, boundary layer, and end effect resistances, respectively, and do not depend on the solute used.

Diffusion of dextran and ficoll was measured in 1.0 μm membranes for determination of D_∞, and 0.015 μm membranes for studies of hindered diffusion. The procedure was similar in each case. Initially 2 mL of tritiated dextran or ficoll solution (6×10^5 CPM/μL) was added to one chamber, with the remaining volume of the two chambers filled with filtered, distilled water. Samples of 0.5 mL were taken from both chambers shortly thereafter and replaced with equivalent volumes of water. Two to four additional samples were taken in this manner at suitable intervals. The duration of the experiments was generally 40-60 min for D_∞ measurements in 1.0 μm membranes, and 6 hr for measurements of D in 0.015 μm membranes. All dextran and ficoll samples were chromatographed on Sephadex G-100 columns and relative concentrations in each fraction determined by scintillation counting (Tri-Carb Model 3375, Packard Instrument Co., Downers Grove, IL), using Aquasol (New England Nuclear) as scintillation fluid. After correcting these concentrations for the dilutions caused by volume replacement, values of C_∞ were obtained by averaging over all samples (one-half the sum of the concentrations). Values of R_T for each fraction were obtained either by averaging R_T values for various sample pairs or by linear regression using Eq. 7, based on all samples in a given experiment. The two approaches generally gave good agreement, and regression coefficients usually exceeded 0.95.

Diffusion of ^{14}C-sucrose, ^{14}C-glucose, or ^{14}C-urea was used for membrane and boundary layer characterization (determination of K_1, K_2, and K_3). The procedure was similar to that described for dextran and ficoll, except that chromatographic fractionation of samples was not required. In these experiments 4-5 samples were usually obtained over a period of 1-3 h. Diffusion of these small solutes was also used to test for dextran or ficoll adsorption in membrane pores, in two types of experiments. One of these involved repeated measurements of ^{14}C-sucrose diffusion across a single 0.015 μm membrane, with both chambers containing either water or equal concentrations of unlabelled dextran or ficoll. Concentrations of unlabelled dextran or ficoll (0.135 g/dL and 0.235 g/dL, respectively) and time of exposure (1-6 h) were similar to those used for diffusion experiments with tritiated macromolecules. In the other adsorption experiments, involving two additional 0.015 μm membranes, diffusion of one of the three small solutes (sucrose, glucose, urea) was measured immediately before and after diffusion experiments with tritiated ficoll or dextran. In either case the object of these experiments was to test for changes in pore radius following exposure of the membrane to dextran or ficoll, as evidenced by changes in R_T.

RESULTS

Characterization of 0.1 μm and 1.0 μm Membranes. Figure 3 shows an electron micrograph of a membrane with 1.0 μm nominal pore diameter. As can be seen, the pores are very nearly circular in cross section. The high porosity of this mem-

TABLE 1. AVERAGE PROPERTIES OF 1.0 μm AND 0.1 μm MEMBRANES

Nominal Pore Diameter (μm)	L(μm)	n(cm^{-2})	r(nm)	$n\pi r^2$
1.0	11.0	1.85×10^7	575	0.192
0.1	5.76	3.32×10^8	67.7	0.0477

TABLE 2. DETERMINATION OF BOUNDARY LAYER RESISTANCE*

Solute	R_T(s/cm)	D_∞(cm²/s)	K_2(cm$^{1/3}$s$^{1/3}$)
Sucrose	2156 ± 68	6.98×10^{-6}	0.144
Glucose	1739 ± 70	9.01×10^{-6}	0.160

* Standard deviations of R_T are based on 6 experiments for sucrose and 5 for glucose.

TABLE 3. CHARACTERIZATION OF 0.015 μm MEMBRANES

Measurement	Membrane 1	Membrane 2
*Sucrose Diff., $R_T(10^4$ s/cm)	7.06 ± 0.42 (4)	8.07 ± 0.76 (4)
*Water Flow, $nr^4/L(10^{-13}$cm²)	6.72 ± 0.46 (12)	4.49 ± 0.12 (8)
Weight, W(g)	0.01426	0.01576
Pore Radius, r(nm)	8.75	7.48
Pore Density, $n(10^8$cm$^{-2})$	7.47	10.4
Pore Length, L(μm)	6.53	7.22
Porosity, $n\pi r^2$	0.00180	0.00182

* The number of time periods for which sucrose diffusion and water flow data were obtained are given in parentheses.

TABLE 4. TESTS FOR DEXTRAN OR FICOLL ADSORPTION IN 0.015 μm MEMBRANES

Membrane No.	Small Solute	Macromolecule	$R_T D_\infty$(cm)	% Change
3	Sucrose	None	0.239	
		None	0.253	+5.9
	Sucrose	None	0.265	
		Dextran	0.256	−3.4
	Sucrose	None	0.284	
		Ficoll	0.300	+5.6
	Sucrose	None	0.272	
		Ficoll	0.269	−1.1
4	Sucrose	None	0.0703	
		Ficoll	0.0714	+1.6
	Glucose	None	0.0655	
		Dextran	0.0679	+3.7
5	Urea	None	0.217	
		Dextran	0.215	−0.9

brane size results in considerable pore overlap on the surface; however, since all pores are not exactly normal to the surface, significantly fewer pores should overlap throughout their entire length. Membranes with nominal pore diameters of 0.1 μm had a similar appearance, except with substantially less pore overlap.

Average characteristics of the 0.1 μm and 1.0 μm membranes are summarized in Table 1. The pore density for 0.1 μm membranes was determined from electron micrographs at 19,400X of a total of 8 samples from 3 membranes. The average number of pores counted was 84.4 ± 5.9 SD, yielding a pore density of 3.32×10^8cm^{-2}. This compares closely with the value of 3×10^8 cm^{-2} quoted by the membrane manufacturer. For the 1.0 μm membranes, 200 ± 5 pores were counted in micrographs of a total of 9 samples at 2900X. The calculated pore density, 1.85×10^7 cm^{-2}, again is close to that quoted (2×10^7 cm^{-2}).

A total of 22 hydraulic permeability measurements were made on 2 of the 0.1 μm membranes, and average weights determined for 6 membranes. The values of pore length and pore radius obtained were $L = 5.76 \pm 0.08$ μm and $r = 67.7 \pm 1.1$ nm. From 5 L_p measurements on 3 of the 1.0 μm membranes, and weights of 2 of these, the corresponding values obtained were $L = 11.0$ μm and $r = 575 \pm 3$ nm. It may be noted that for these two membrane sizes, our average measured pore radii are substantially larger than the nominal values (67.7 vs. 50 nm, and 575 vs. 500 nm).

Determination of the Boundary Layer Resistance. The boundary layer resistance, as expressed by the constant K_2 in Eq. 13, was determined by measurements of total resistance (R_T) of 0.1 μm membranes to small solutes of known diffusivity (sucrose and glucose). The average pore radius of these membranes (67.7 nm) is much larger than the Stokes-Einstein radii of these two solutes (0.47 nm for sucrose and 0.36 nm for glucose), so that steric and hydrodynamic hindrances to diffusion should be negligible, and $D \simeq D_\infty$ in Eq. 13. The constants K_1 and K_3 may be evaluated from the data in Table 1 (1.21×10^{-2} cm and 2.23×10^{-4} cm, respectively), leaving K_2 as the only unknown in Eq. 13. Results are shown in Table 2. The values of R_T are based on 6 sucrose experiments in 3 membranes and 5 glucose experiments in 2 membranes. In these experiments the boundary layer resistance ($2R_b$) for either solute is about 20% of R_T, the end effects being minor ($2R_e$, ~2%) and the remainder being due to the membrane (R_m, ~80%). The standard deviations of R_T shown in Table 2 are about 3-4% of the mean values, so that the corresponding uncertainty in K_2 is ±15-20%. The values of K_2 from the sucrose and glucose data, 0.144 and 0.160 (cm · s)$^{1/3}$, respectively, are in agreement within this estimate of experimental error, and an average value of 0.152 (cm · s)$^{1/3}$ was therefore used in all subsequent calculations. It may be noted that the corresponding mass transfer coefficients (k) for su-

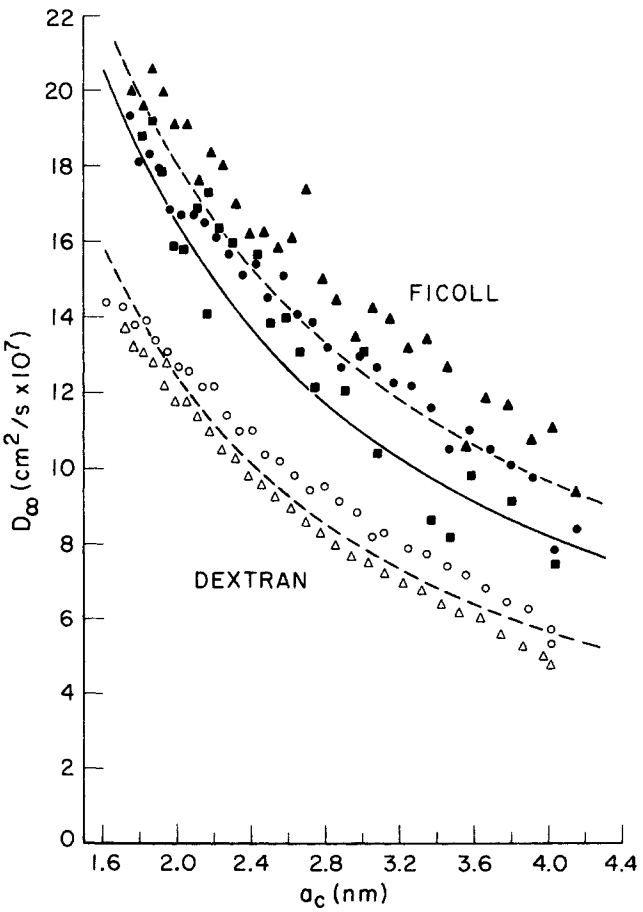

Figure 4. Free diffusivity for dextran and ficoll as a function of molecular radius from gel chromatography. Each set of symbols represents one experiment. The solid curve is based on Eq. 1 using $a = a_c$; the dashed curves are from least squares fits, Eqs. 14 and 15.

crose and glucose are about twice those predicted from the correlation of Colton and Smith (1972) at our cell Reynolds number (1.6×10^4). Such differences are not unexpected since in Eq. 12 the constant α, in particular, is dependent on the details of the stirrer and cell configuration.

Characterization of 0.015 μm Membranes. As already noted, the resolution of the scanning electron micrographs was insufficient for determination of pore density in membranes with 0.015 μm nominal pore diameters. Accordingly, sucrose diffusion measurements were employed, together with weighing and hydraulic permeability determination. Values of n, r, and L were calculated from the measured values of W, L_p, R_T and K_2 using Eqs. 5, 6 and 13. The two 0.015 μm membranes used in the dextran and ficoll hindered diffusion experiments, referred to as membranes 1 and 2, were individually characterized by performing the above three measurements on both. Results are summarized in Table 3. Although these membranes were from the same lot, it can be seen that there are significant differences in all three measured properties. The most striking of these is a 50% larger hydraulic permeability in membrane 1 than in membrane 2. These differences are reflected in the calculated values of pore radius, pore density, and pore length. The pore radius for membrane 2 is equal to the nominal value (7.48 nm) while that for membrane 1 is 17% larger (8.75 nm). Porosities of the two membranes were essentially identical, however. For these membranes the ratio of sucrose Stokes-Einstein radius to pore radius was 0.054-0.063, large enough for there to be a substantial hindered diffusion effect, as predicted by Eqs. 3 or 4. This was taken into account by calculating D/D_∞ with Eq. 4 for use in Eq. 13; values obtained were 0.741 for membrane 1 and 0.708 for membrane 2. If this correction were ignored, calculated pore radii would be substantially larger (10.17 vs. 8.75 nm and 8.89 vs. 7.48 nm). It may be noted that in the sucrose diffusion experiments the sum of the calculated resistances due to boundary layer and end effects is only 0.5-0.6% of the total resistance, so that R_m is essentially equal to the measured value of R_T.

Tests for Dextran or Ficoll Adsorption. Significant adsorption of dextran or ficoll in membrane pores would make interpretation of the macromolecule diffusion experiments difficult, so that this possibility was examined in a separate set of experiments. In these, diffusion of small solutes was measured in three membranes with 0.015 μm nominal pore diameters, with the results shown in Table 4. Experiments with membrane 3 were performed before and during exposure of the membrane to solutions of unlabelled dextran or ficoll; pairs of measurements shown were done on succeeding days (membranes rinsed and stored in water overnight), both measurements in a pair being done on the same day. For membranes 4 and 5, diffusion of small solutes was measured before and after a dextran or ficoll diffusion experiment of several hours duration. Total membrane resistance in Table 4 is expressed as $R_T D_\infty$. As already noted, $R_T \simeq R_m$ for these small pore sizes, so that $R_T D_\infty \simeq (L/n\pi r^2)(D_\infty/D)$. Thus, decreases in pore radius resulting from dextran or ficoll adsorption would be reflected by increases in $R_T D_\infty$. As can be seen in Table 4, changes in $R_T D_\infty$ following addition of dextran or ficoll were apparently random and did not exceed ±6%. Corresponding changes in calculated pore radius are less than ~0.3 nm. As indicated by the first pair of values in Table 4, which serve as a control (no macromolecule added), and the data on R_T in Table 3, the extent of variation seen is that expected from the reproducibility of the R_T measurements. Membrane 4 is from a different lot than membranes 1, 2, 3 and 5, and the low resistance seen with either solute is representative of other membranes in that lot. We conclude that significant amounts of dextran or ficoll are not adsorbed in the pores of these polycarbonate track-etch membranes. Based on water flow data in similar membranes, Schultz et al. (1979) also found little or no change in pore radius with dextran solutions, but substantial changes with solutions of various proteins.

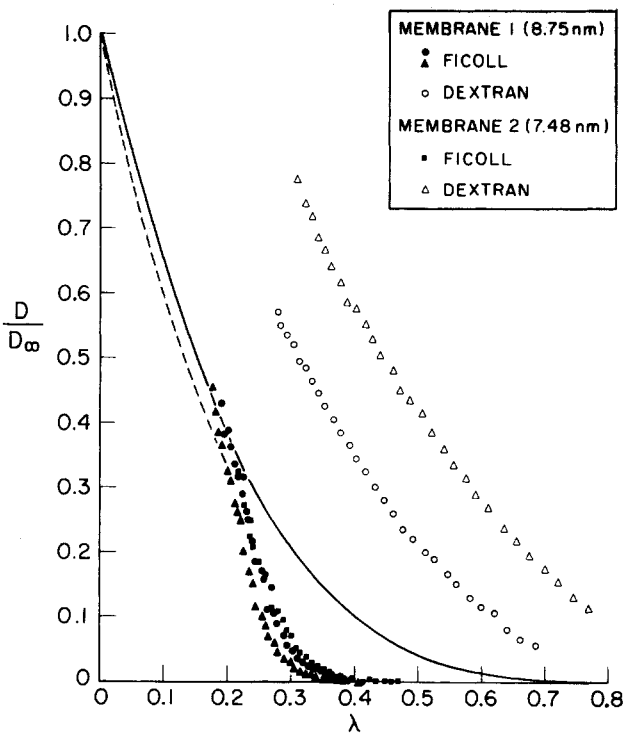

Figure 5. Ratio of pore-to-bulk diffusivities for dextran and ficoll as a function of the ratio of Stokes-Einstein radius to pore radius. Each set of symbols represents one experiment. The solid curve is calculated from Eq. 3 using $f(\lambda, 0)$ from Paine and Scherr (1975), the dashed curve from Eq. 4.

Measurement of Free Diffusivities for Dextran and Ficoll. Values of D_∞ for dextran and ficoll were determined from diffusion experiments in membranes with pore diameters sufficiently large (1.0 μm nominal) to insure that $D \simeq D_\infty$; ratios of effective molecular radius to pore radius in this case were <0.01. In these experiments the boundary layer and end effects accounted for ~20% and ~6% of R_T, respectively, the remainder being due to the membrane resistance. Results of three experiments with ficoll and two with dextran are shown in Fig. 4, where D_∞ is plotted against the molecular radius determined from gel chromatography (a_c). At any given "column radius," the diffusivity of ficoll is significantly greater than that of dextran. The solid curve is a plot of Eq. 1 assuming equality of the column and Stokes-Einstein radii. Equating these two measures of molecular size is apparently a better approximation for ficoll than for dextran.

The dashed curves in Figure 4 represent least-squares fits to the data using power law expressions. These equations are

$$D_\infty = (2.675 \times 10^{-6}) a_c^{-1.112} \quad \text{(dextran)} \tag{14}$$

$$D_\infty = (3.345 \times 10^{-6}) a_c^{-0.893} \quad \text{(ficoll)} \tag{15}$$

where D_∞ is in cm²/s and a_c is in nm. Neither exponent of a_c differs significantly from −1.0, the 95% confidence limits being -1.112 ± 0.299 and -0.893 ± 0.218.

Hindered Diffusion of Dextran and Ficoll. Results of five hindered diffusion experiments, three with ficoll and two with dextran, are shown in Figure 5. The Stokes-Einstein radius was chosen here as the more appropriate measure of molecular size in calculating λ. Values of D/D_∞ for ficoll tend to be very consistent with one another, whether obtained with successive experiments on the same membrane or with different membranes. The results obtained for dextran in the two membranes are less consistent with one another, but are clearly different than those for ficoll. Theoretical predictions of Eqs. 3 and 4, based on hard sphere models, are shown by the solid and dashed curves, respectively. At any given molecular radius, values of D/D_∞ for dextran substantially exceed the theoretical

predictions, while those for ficoll are at or below the theoretical calculations. If column radius were used in calculating λ rather than Stokes-Einstein radius, there would be less difference between the dextran and ficoll curves, but still no overlap. For example, the extreme values of λ for dextran would shift from about 0.30 to 0.23 and about 0.75 to 0.52; the extremes for ficoll would change less, from about 0.20 to 0.22 and 0.45 to 0.53. Values of D/D_∞ for dextran would continue to exceed those for ficoll over the entire range of λ studied.

DISCUSSION

The interpretation of the hindered diffusion results is of course dependent on the various measurements used in membrane characterization, determination of boundary layer resistances, and evaluation of free diffusivity for dextran and ficoll. Of the various quantities calculated, the boundary layer constant, K_2, is probably known with the least precision. Since in the sucrose experiments with 0.1 μm membranes the boundary layer resistance was only about 20% of R_T, errors made in the measurement of R_T are amplified. We estimate the uncertainty in R_T in these experiments to be about 4%, giving about a 20% uncertainty in total boundary layer resistance and the coefficient K_2. This situation could be improved in principle by employing membranes with lower resistance (larger pore size), which would make the boundary layer resistance a larger fraction of the total. This was avoided since the larger porosities of such membranes result in significantly more pore overlap, thereby causing difficulties in the interpretation of water flow measurements (see below). Fortunately, the boundary layer resistance is calculated to be only about 20% of the total for dextran or ficoll diffusion in 1.0 μm membranes, and less than 1% for diffusion of any of the solutes in 0.015 μm membranes. Thus, even 20% uncertainties in boundary layer resistance have little effect on the D/D_∞ results for dextran and ficoll.

The determination of D_∞ for dextran and ficoll is probably less accurate than that of D. The relatively frequent pore overlap seen in the 1.0 μm membranes (Figure 3) used for D_∞ measurements creates a possible systematic error in evaluating the pore radius from water flow measurements. In assuming uniform pores, as in Eq. 6, the tendency will be to overestimate porosity (total cross sectional area of all pores). This is the quantity needed in evaluating D_∞, since for nonisoporous membranes it takes the place of $n\pi r^2$ in Eqs. 9 and 11 for the coefficients K_1 and K_3. The probable error is difficult to evaluate precisely, but from the observed degree of pore overlap and some rather crude calculations based on the hydraulic radius concept, it appears that porosity may be overestimated on the order of 10%. If this is the case, the values of D_∞ shown in Figure 4 and correlated in Eqs. 14 and 15 may be about 10% too low. This problem is mitigated to some extent by the likelihood that relatively few pores that overlap on the membrane surface will continue to overlap along their entire length, since they are not all normal to the surface. For this reason, and because of the difficulty in establishing any correction factor with precision, we have chosen not to modify any of the measured values of D_∞. This source of error clearly does not influence the comparison of D/D_∞ values for dextran and ficoll, since D_∞ values for both series of macromolecules would be affected equally. The D/D_∞ values obtained from three hindered diffusion experiments with ficoll are quite consistent with one another, while results from the two dextran experiments show a substantial discrepancy. We have been unable to identify the reason for this discrepancy; possible explanations for a shift in the entire D/D_∞ vs. λ curve include contamination leading to blockage of some pores in one of the membranes, an undetected change in the elution characteristics of the gel column used in fractionating the samples, or an improper temperature setting in the diffusion cell during one of the runs.

Our finding that D/D_∞ for dextran significantly exceeds that for ficoll of comparable radius is consistent with several reports in the literature comparing transport of relatively rigid macromolecules with macromolecules expected to behave more like flexible, random coils. In a previous study using these same macromolecules, Bohrer et al. (1979) compared ultrafiltration rates of dextran and ficoll across the walls of glomerular capillaries of rat kidneys in vivo. In analogy with the present findings, normalized filtration rates of dextran exceeded those of ficoll at any given column radius; replotting of those results using Stokes-Einstein radii determined from the present study would cause the difference to be even greater. Colton et al. (1975) examined diffusion and equilibrium partitioning of several macromolecules in a leached borosilicate glass reported to have a narrow pore size distribution. Solutes studied were two proteins in aqueous solution and nearly monodisperse polystyrene fractions in chloroform and dichloroethane. An enhanced drag effect ($f > f_\infty$ in our notation) was noted for the relatively compact and rigid proteins, but not for the polystyrene fractions. Thus, the effective diffusivities of polystyrenes in pores were interpreted as being reduced as a result of partitioning only ($\phi < 1$ but $f = f_\infty$). In additional experiments related to molecular configuration, Laurent et al. (1963, 1975) studied the sedimentation of various proteins and linear polymers through hyaluronic acid gels. They found that for molecules of equivalent Stokes-Einstein radii, the linear polymers had a greater sedimentation rate through the gel matrix than the globular proteins. They postulate that these differences in sedimentation rates are due to differences in molecular configuration among these various macromolecules.

In each of the previous studies just discussed the porous medium used (capillary wall, porous glass, hyaluronate gel) has a relatively complex structure, and comparison of results with theoretical predictions is difficult. This complication was avoided by Schultz et al. (1979), who measured the osmotic reflection coefficient (σ) for a variety of proteins and several dextran fractions using track-etch polycarbonate membranes of various pore sizes. Increasing values of σ are evidence of greater hindrance to convective solute transport. For a given molecular size, σ values for proteins significantly exceeded those for dextrans. Although scatter in the data precluded a precise comparison with σ values predicted from hydrodynamic theories of hindered transport, σ values for proteins tended to follow the theoretical predictions while those for dextran were markedly lower.

Our results and those of Schultz et al. (1979) both indicate that in membrane pores dextran behaves as if it has an equivalent radius much less than (roughly one-third to one-half) its Stokes-Einstein radius. To the extent that this is related to the ability of dextran to deform, it is apparent that shear-induced deformation within pores is not required, since in our experiments there was no transmembrane water flow. Alternatively, as suggested by Colton et al. (1975) for polystyrene, it is possible that for dextrans there is little added frictional hindrance ($f \approx f_\infty$), but only a partitioning effect ($\phi < 1$) leading to $D/D_\infty < 1$ (Eq. 2). This would be true if dextrans behaved as free draining macromolecules, in which the frictional length scale would be more closely approximated by the size of a monomer than by the size of the polymer coil. Recent measurements of electrophoretic mobilities of dextran sulfate and diethylaminoethyl dextran are consistent with free draining behavior (Deen et al., 1980).

We expect that the crosslinked structure of ficoll will cause it to be much more rigid than dextran. Calculations based on the theory of Scheraga and Mandelkern (1953) for rigid ellipsoidal particles, using measurements of intrinsic viscosity, partial specific volume, and sedimentation coefficient, yield effective axial ratios for ficoll between 1 and 2 (Bohrer et al., 1979). Thus, it appears that ficoll may be reasonably approximated as a solid sphere, although other models, such as a rigid but porous sphere, are not excluded. Our finding that D/D_∞ for ficoll is generally lower than predicted by Eq. 3 (solid curve, Figure 5) may be explained in part by the fact that the replacement of the radial average of $f^{-1}(\lambda, \beta)$ with $f^{-1}(\lambda, 0)$, in obtaining Eq. 3 from Eq. 2, leads to overestimates of D/D_∞. The magnitude of the error for small λ is indicated by comparison of Eqs. 3 and 4

(Figure 5), the latter being more exact for $\lambda << 1$. More complete results for $f(\lambda, \beta)$ are required to determine whether the discrepancy between Eq. 3 and D/D_∞ measurements for ficoll for $\lambda > 0.2$ is due to the approximate evaluation of the frictional coefficient in Eq. 3, or the failure of ficoll to behave as a solid sphere.

ACKNOWLEDGMENTS

This work was supported by grants from the Whitaker Health Sciences Fund, the National Institutes of Health (Biomedical Research Support Grant 5-S-07-RR07047-14) and the National Science Foundation (ENG-7905576).

NOTATION

a = solute radius from Stokes-Einstein equation, Eq. 1
a_r = estimate of solute radius from gel chromatography
A = exposed membrane area in diffusion cell
A_T = total membrane area
b = radius of exposed membrane in diffusion cell
C = solute concentration in "downstream" chamber during batch diffusion run; $C = C_0$ at $t = 0$ and $C = C_\infty$ at equilibrium
D = apparent diffusion coefficient in membrane pores
D_∞ = diffusion coefficient in bulk solution
f = molecular friction coefficient in membrane pores
f_∞ = molecular friction coefficient in bulk solution, Eq. 1
k = mass transfer coefficient for boundary layer
$\hat{k}$ = Boltzmann's constant
K_1, K_2, K_3 = empirical constants in Eq. 13
L = average pore length
L_p = membrane hydraulic permeability, defined by Eq. 6
n = number density of pores
N_{Re} = Reynolds number based on stirring speed and membrane radius
N_{Sc} = Schmidt number
ΔP = hydrostatic pressure difference across membrane
Q = volumetric flow rate across membrane
R = mass transfer resistance, R_T for total, R_m for membrane, R_b for boundary layer, and R_e for end effects
r = pore radius
t = time
T = temperature
V = volume of one chamber of diffusion cell
W = mass of membrane

Greek Letters

α, γ = dimensionless empirical constants in correlation for mass transfer coefficient, Eq. 12
β = dimensionless radial coordinate, relative to pore radius
λ = ratio of Stokes-Einstein radius to pore radius, a/r
μ = viscosity of water
ρ = density of polycarbonate
σ = osmotic reflection coefficient
ϕ = equilibrium partitioning coefficient, Eq. 2
ϵ = volume fraction of solute

LITERATURE CITED

Anderson, J. L., "Prediction of the Concentration Dependence of Macromolecular Diffusion Coefficients," *Ind. Eng. Chem. Fundam.*, **12**, 448 (1973).

Anderson, J. L. and J. A. Quinn, "Restricted Transport in Small Pores: A Model for Steric Exclusion and Hindered Particle Motion," *Biophys. J.*, **14**, 130 (1974).

Bean, C. P., "The Physics of Porous Membranes—Neutral Pores," *Membranes*, G. Eisenman, ed., New York, Marcel Dekker, Inc., **1**, p. 1 (1972).

Beck, R. E. and J. S. Schultz, "Hindrance of Solute Diffusion within Membranes as Measured with Microporous Membranes of Known Pore Geometry," *Biochim. Biophys. Acta*, **255**, 273 (1972).

Bohrer, M. P., W. M. Deen, C. R. Robertson, J. L. Troy, and B. M. Brenner, "Influence of Molecular Configuration on the Passage of Macromolecules across the Glomerular Capillary Wall," *J. Gen. Physiol.*, **74**, 583 (1979).

Brenner, H. and L. J. Gaydos, "The Constrained Brownian Movement of Spherical Particles in Cylindrical Pores of Comparable Radius," *J. Colloid Interface Sci.*, **58**, 312 (1977).

Chang, R. L. S., I. F. Ueki, J. L. Troy, W. M. Deen, C. R. Robertson, and B. M. Brenner, "Permselectivity of the Glomerular Capillary Wall to Macromolecules: II. Experimental Studies in Rats Using Neutral Dextran," *Biophys. J.*, **15**, 887 (1975).

Colton, C. K., C. N. Satterfield, and C.-J. Lai, "Diffusion and Partitioning of Macromolecules within Finely Porous Glass," *AIChE J.*, **21**, 289 (1975).

Colton, C. K. and K. A. Smith, "Mass Transfer to a Rotating Fluid: Part II., Transport from the Base of an Agitated Cylindrical Tank," *AIChE J.*, **18**, 958 (1972).

Conlon, T. and B. Craven, "Hindering of Diffusion by Pores," *Aust. J. Chem.*, **25**, 695 (1972).

Deen, W. M., M. P. Bohrer, and B. M. Brenner, "Macromolecule Transport across Glomerular Capillaries: Application of Pore Theory," *Kidney Int.*, **16**, 353 (1979).

Deen, W. M., B. Satvat, and J. M. Jamieson, "Theoretical Model for Glomerular Filtration of Charged Solutes," *Am. J. Physiol.*, **238**, F126 (1980).

Granath, K. A., "Solution Properties of Branched Dextrans," *J. Colloid Sci.*, **13**, 308 (1958).

Larm, O., B. Lindberg, and S. Svensson, "Studies on the Length of the Side Chains of the Dextran Elaborated by Leuconostoc Mesenteroides NRRL B-512," *Carbohydrate Res.*, **20**, 39 (1971).

Laurent, T. C., I. Björk, A. Pietruszkiewicz, and H. Persson, "On the Interaction between Polysaccharides and Other Macromolecules. II. The Transport of Globular Particles through Hyaluronic Acid Solutions," *Biochim. Biophys. Acta*, **78**, 351 (1963).

Laurent, T. C., B. N. Preston, H. Pertoft, B. Gustafsson, and M. McCabe, "Diffusion of Linear Polymers in Hyaluronate Solutions," *Eur. J. Biochem.*, **53**, 129 (1975).

Liabastre, A. A. and C. Orr, "An Evaluation of Pore Structure by Mercury Penetration," *J. Colloid Interface Sci.*, **64**, 1 (1978).

Malone, D. M. and J. L. Anderson, "Diffusional Boundary-Layer Resistance for Membranes with Low Porosity," *AIChE J.*, **23**, 177 (1977).

Malone, D. M. and J. L. Anderson, "Hindered Diffusion of Particles through Small Pores," *Chem. Eng. Sci.*, **33**, 1429 (1978).

Paine, P. L. and P. Scherr, "Drag Coefficients for the Movement of Rigid Spheres through Liquid-Filled Cylindrical Pores," *Biophys. J.*, **15**, 1087 (1975).

Price, P. B. and R. M. Walker, "Chemical Etching of Charged-Particle Tracks in Solids," *J. Appl. Phys.*, **33**, 3407 (1962).

Prieve, D. C. and P. M. Hoysan, "Role of Colloidal Forces in Hydrodynamic Chromatography," *J. Colloid Interface Sci.*, **64**, 201 (1978).

Scheraga, H. A. and L. Mandelkern, "Consideration of the Hydrodynamic Properties of Proteins," *J. Am. Chem. Soc.*, **75**, 179 (1953).

Schultz, J. S., R. Valentine and C. Y. Choi, "Reflection coefficients of Homopore Membranes: Effect of Molecular Size and Configuration," *J. Gen. Physiol.*, **73**, 49 (1979).

Silebi, C. A. and A. J. McHugh, "An Analysis of Flow Separation in Hydrodynamic Chromatography of Polymer Latexes," *AIChE J.*, **24**, 204 (1978).

Smith, F. G. and W. M. Deen, "Electrostatic Double Layer Interactions for Spherical Colloids in Cylindrical Pores," *J. Colloid Interface Sci.*, **78**, 444 (1980).

Van Bruggen, J. T., J. D. Boyett, A. L. van Bueren, and W. R. Galey, "Solute Flux Coupling in a Homopore Membrane," *J. Gen. Physiol.*, **63**, 639 (1974).

Wong H., J. and J. A. Quinn, "Hindered Diffusion of Macromolecules in Track-Etched Membranes," *Colloid and Interface Science*, M. Kerker, ed., Academic Press, New York, **5**, p. 169 (1976).

Manuscript received September 10, 1980; revision received December 15, and accepted December 23, 1980.